Unsteady thin film flow of a hybrid nanoliquid with magnetic effects

Kakanuti Malleswari
Department of Mathematics, MREC, Medchal Mandal, India and Department of Applied Mathematics, SPMVV, Tirupati, India, and
Sarojamma G.
Department of Applied Mathematics, Sri Padmavati Mahila Visvavidyalayam, Tirupati, India

Abstract

Purpose – This study aims to explore the thermal energy diffusion and flow features of a hybrid nanofluid in a thin film. In particular, the focus is to elicit the impact of shape factor in the backdrop of a magnetic field. The hybrid nanofluid is the amalgamation of various shaped nanoscale particles of copper and alumina in water.

Design/methodology/approach – The equations of motion and energy are modeled using the Tiwari–Das model. The differential equations governing the physics of the designed model have been obtained by the application of scaling analysis. To achieve quantitative outcomes, Runge–Kutta–Fehlberg numerical code along with shooting techniques is used. Validation of the derived outcomes with available data in literature reveals a greater accuracy of the numerical procedure used in this investigation.

Findings – The dynamics of the slender nano liquid film is explored eliciting the impact of various flow parameters. The rate of energy transport of the Cu-Al_2O_3/ water with blade-shaped nanoparticle, at a fixed Prandtl number (=2) is enhanced by 14.7% compared to that evaluated with spherical particles. The presence of hybrid nanoparticles has an affirmative impact in boosting the rate of heat transfer (RHT). The temperature and the rate of thermal diffusion of the hybrid nanofluid are more prominent than those of the Cu-H_2O case. The numerical outcomes of this investigation are collated with the already published works as a limiting case and are found to be in good agreement.

Originality/value – The adopted methodology helped to obtain the results of the present problem. To the best of authors' knowledge, it can be shown that the originality of the work with the table of comparison. There is a good agreement between present outcomes with the existed results.

Keywords Thin film flow, Unsteady flow, Film thickness, MHD, Hybrid nanofluid, Heat transfer, Shape factor

Paper type Research paper

Nomenclature

Roman letters

(b, c) = positive constants;
B_0 = constant magnetic strength;
C_p = specific heat at constant pressure;
f = dimensionless stream function;
k = thermal conductivity of the fluid;
M = magnetic field parameter = $\frac{\sigma f B_0^2}{b\rho f}$;
Pr = Prandtl number = $\frac{(\mu C_p)f}{k_f}$;
Re_x = Reynolds number= $\frac{Ux}{v}$;
S = unsteadiness parameter = $\frac{c}{b}$;
S_f = shape factor;
T = fluid temperature;
T_∞ = ambient fluid temperature;
T_0 = temperature at the slit; and
(u, v) = velocity components along x, y-axis.

Greek symbols

μ = dynamic viscosity;
v = kinematic viscosity;
ρ = fluid density;
σ = electrical conductivity;
ϕ_1 = volume fraction of copper;
ϕ_2 = volume fraction of alumina;
$_\theta$ = dimensionless temperature;
B = specific heat capacity; and
ξ = film thickness.

Subscript

nf = nanofluid;
hnf = hybrid Nanofluid;
f = fluid;
s_1 = copper; and
s_2 = alumina.

Superscript

$'$ = differentiation with respect to η.

The current issue and full text archive of this journal is available on Emerald Insight at: **https://www.emerald.com/insight/1708-5284.htm**

World Journal of Engineering
© Emerald Publishing Limited [ISSN 1708-5284]
[DOI 10.1108/WJE-01-2024-0043]

Received 29 January 2024
Revised 8 April 2024
Accepted 1 May 2024

1. Introduction

The 21st century has witnessed a significant surge in scientific and technological discoveries and innovations. One among these innovations is modeling of nano fluid (NF). NFs find applications in enhancing heat transfer efficiency, drug transport, oncological therapy, etc. The innovation of Choi and Eastman (1995) in enhancing the thermal conductivity (TC) of traditional fluids is a breakthrough in heat transfer applications. They accomplished it by amalgamating the nano-scaled solid particles in these conventional materials such as water, ethylene glycol and engine oil. They coined these mixtures of nanomaterials and liquids carrying these nanoparticles as nanofluids. Experimental studies (Choi and Eastman, 1995; Eastman *et al.*, 2001) affirmed the thermal diffusivity of these amalgamated liquids show a very promising enhancement over the traditional fluids. To model the nanofluid dynamics, two approaches are followed; one approach is proposed by Buongiorno (2006) which includes Brownian motion and thermophoresis which are emphasized to be responsible for the augment of the thermal properties of the NFs. The second approach is suggested by Tiwari and Das (2007). It is based on the effective medium theory, describes the density, heat capacity, thermal diffusivity, etc. in terms of the corresponding properties of the used nanoparticles and base liquid. Following these two models, all researchers explored the flow heat transfer characteristic of NFs (Khan and Pop, 2010; Bachok *et al.*, 2012; Hassan *et al.*, 2018; Sheikholeslami and Sadoughi, 2018). Sreelakshmi *et al.* (2019) examined the influence of microconvection and thermophoresis on the stagnation point radiative flow of a Jeffrey nanofluid. The coupled impact of chemical reaction, phase change heat transmission, viscous heating under the action of the Lorentz force is included. Their findings are that the Debora number and parameter of melting heat enhanced the velocity. Thermal measure is elevated with thermophoresis, Prandtl and Eckert numbers, while parameters of radiation and Brownian motion have a declining influence. Buongiorno and Hu (2010) discussed the augmented properties of nanofluids in nuclear reactor applications. Bachok *et al.* (2010) explored the nanoliquid flowing steadily on a moving surface in a uniform free stream. Nadeem *et al.* (2014) obtained the attributes of thermal energy in a nano liquid over a surface that elongates exponentially. Three types of nano liquids are considered by dispersing Cu, alumina and TiO_2 nano-sized particles in H_2O.

Scientists pursued investigations to enhance the thermophysical characteristics of base fluids beyond the improvements achieved with nanofluids. This expected enhancement is accomplished by considering the dispersion of two distinct nano-scaled particles in a base liquid and this amalgamated mixture is coined as "Hybrid nanofluid (HNF)." Turcu *et al.* (2006) and Jana *et al.* (2007) appear to be the pioneering researchers to conduct experimental studies using nanocomposite particles. Several of the studies on HNF (Devi and Devi, 2016, 2017; Ghadikolaei *et al.*, 2018, 2019) indicate that the rate of thermal energy transport in HNF is superior to that in mono nanofluid (MNF). Veera Krishna *et al.* (2021) deliberated the chemically reactive radiative unsteady flow of an HNF [Ag-Ti O_2/(H_2O-$C_2H_6O_2$)] streaming past a reference exponentially accelerated moving porous vertical moving porous plate within a rotating frame. They found that the resultant velocity is augmented for advanced values of temperature and concentration buoyant forces, whereas parameters of rotation and slip have a reversal effect. Further Ag-Ti O_2/(H_2O-$C_2H_6O_2$) HNF is found to possess higher thermal measure than that of the Ag/(H_2O-$C_2H_6O_2$) fluid.

Manjunatha *et al.* (2019) explored the enhancement of heat flow characteristics in a free convective hybrid nanofluid subjected to a Lorentz force assuming the viscosity to be temperature-dependent. The numerical solutions suggest that the TC of the hybrid NF (Al_2O_3-Cu/H_2O) exceeds that of the mono-phasic nanofluid Cu/H_2O. Diminishing variable viscosity shows a decreasing trend in the thickness of the boundary layers of both hybrid and MNFs. Adopting Buongiorno's model, Bhatti *et al.* (2022) analyzed the flow features of a HNF (Ti O_2 – Cu O/H_2O) streaming past an elastic flat surface using the Keller box numerical algorithm. The repercussions of Joule heating, viscous dissipation, temperature and wall slips are taken into consideration. They reported that the presence of hybrid nanoparticles leads to increased fluid velocity, thermal measure and concentration. The micro convection and thermophoretic force contribute to elevating temperatures. Higher Schmidt's number corresponds to decreased concentration. Selimefendigil and Oztop (2023) evaluated the performance of convective thermal transfer on an HNF and flow for multi-jet impingement system containing phase-change-packed bed (PCM-PB) subjected to the Lorentz force. Their numerical outcomes indicate that spatial average Nusselt number (Nu). PCM+nanoliquid has a 13.5% higher measure than that of pure liquid for the highest magnetic field (MgF) strength. Thamizhselvi *et al.* (2023) assessed the heat and flow features of a radiative HNF in an asymmetric channel through a non-Darcy porous matrix. They explored the repercussions of activation energy, varying TC and heat source subjected to convective boundary constraints for temperature and concentration. The HNF consists of the single and multi-wall nanotubes merged in the host liquid ethylene glycol. They concluded that the heat transmission rate of the HNF at the lower boundary is 5.8% greater relative to that of the base fluid for a variation in variable TC number. The HNF has a 20% higher rate of species concentration than that of the base liquid with activation energy parameter.

Of late, researchers focus on the studies of flows in thin films because of their numerous functional applications across various industrial sectors. Film flow refers to the presence of a liquid layer with one free surface and the other moveable owing to external forces such as shear stress or gravity. Modeling of this phenomenon can be applied in industries such as coatings and high-performance capacitors and cable and wire coating. Moreover, it plays a crucial role in the manufacturing of micro-electronic components such as hard drives, screens, electronic circuits and microchips. In all coating procedures, it is imperative to achieve a smooth and glossy surface on the final artifact, ensuring the highest quality finish regarding strength, transparency and minimal friction. This guarantees that the end product distinguishes itself in the market with an appearance and optimal efficiency. Wang (1990) pioneered the analysis of flow dynamics within a thin film on an elastic surface, deriving both asymptotic and numerical solutions. Further, he derived an expression for film thickness involving unsteadiness parameter. Following this analysis, several researchers (Nadeem and Awais, 2008; Abel *et al.*, 2009; Vajravelu *et al.*, 2012; Megahed, 2015; Sarojamma *et al.*, 2017; Ullah *et al.*, 2018; Sreelakshmi and Sarojamma, 2018)

investigated the flow and thermal energy characteristics within a thin film on elongated surfaces under various conditions encompassing both Newtonian and non-Newtonian liquid behavior.

The first analysis to discuss the thin film problem in NFs is by Narayana and Sibanda (2012). They analyzed the flow dynamics of a nano liquid in a slender film on an elongated surface using effective medium theory. They observed thickness of the film decreases with nanoparticle volume fraction in Cu-H_2O nanofluid while the opposite is noted in Al_2O_3 with H_2O nano liquid. Increasing volume fraction of the nanoscale particles yielded thicker thermal boundary layers in both phases. Xu *et al.* (2013) explored the thermal energy characteristics and flow behavior of a nano liquid thin film. They considered three types of nanofluids Cu- H_2O, Al_2O_3 -H_2O and TiO_3 -H_2O. Their HAM outcomes elicit that film thickness is drastically declined with increased unsteadiness. Adil Sadiq (2021) extended the work of Narayan and Sibanda by including the internal heat generation and solved problem using HAM and concurred with the observation of Narayana and Sibanda (2012). Leong *et al.* (2020) made a computational investigation of the thin film flow behavior of a hybrid nano liquid on an elastic sheet with a specific consideration given to thermo-capillarity. Anantha Kumar *et al.* (2019) addressed the repercussions of non-uniform heat source and sink and thermal radiation within the thin film of a hybrid nano liquid (Co. $Fe_2O_4 - Fe_3O_4$/(H_2O-EG). Their numerical outcomes inferred that the thickness of the film declines flow velocity and thermal measure. Gul *et al.* (2020) deliberated the slender film flow of the HNF(CNT-Fe_3O_4-H_2O) through a stretching cylinder subjected to a magnetic field using HAM. They reported that the impact of multi-walled and single-walled CNTs is more pronounced in comparison to Fe_3O_4 nanoparticles. Alharbi *et al.* (2024) expounded the 3D steady nano liquid (Cu-Al_2O_3/H_2O) thin film flow over an inclined spinning disk inserted in a porous medium. Their graphical plots obtained by using HAM enlighten that the presence of a porous medium accelerated the rate of energy transmission. Velocity and rate of thermal transmission declined with increased thickness of the film. Jazaa *et al.* (2024) explored the enhanced energy characteristics and flow features and entropy generation of a partially ionized liquid thin film flow of a nanoliquid (ZnO-Al_2O_3/Powell–Eyring liquid) in the backdrop of heat generation and magnetic force. Their results indicate that film thickness is reduced for increased magnetic number. The entropy followed a decreasing trend with parameters of unsteadiness, ion slip and Hall current.

The geometry of the nanoparticles significantly impacts the nanofluid exerting a prominent influence on its productive TC and heat efficiency of the NF. Categorically, nanoparticles with different shapes show varying levels of surface - to - efficiency of volume ratio, influencing the thermal transmission. Analysis of the impact of shape factor enables the scientists to develop thin film nanofluid flow for certain industrial applications such as solar thermal collectors and cooling of microelectronics. The objective of the present study is to explore the enhancement of the TC of the HNF and MNF, focusing particularly, on how the shape factor influences efficiency of the energy transport.

Novelty of the research communication:

This research study will address the following issues:

- What role do the shape factor and volume fraction of nanoparticles play in influencing temperature within the fluids, and how do these factors contribute to enhancing thermal properties?
- How do the velocity profiles of the studied fluids change with variations in parameters M, ϕ and S?
- What is the significance of the observed temperature difference between the HBF and MNF, and how does it relate to the overall thermal behavior of these fluids?
- How does skin friction at the boundary vary with changes in S and M, and what are the implications of these variations on the fluid dynamics?

2. Mathematical framework

The study examines the transient laminar flow of an incompressible HNF comprising water (H_2O) as the host fluid with copper (Cu) and aluminum oxide (Al_2O_3) nanoscale particles, flowing in a film of thickness h on an elongated surface. The thermophysical characteristics of the HNF are regarded as constant. A MgF of variable intensity $B = B_0(1-ct)^{-1/2}$ is enforced in the normal direction to the surface. The sheet's geometry and directions of the fluid motion are depicted in Figure 1. Assuming a small-scale magnetic Reynolds number, the MgF's induced effect is ignored. The flow commences as a result of the elongation of the sheet. The velocity of elongation is taken as $U(x,t) = \frac{bx}{1-ct}$. It is assumed that surface tension exerts an insignificant influence on the flow.

With these assumptions, the flow within the slender film is represented by the equations (Wang, 1990; Anantha Kumar *et al.*, 2019):

$$\frac{\partial u}{\partial x} + \frac{\partial v}{\partial y} = 0, \tag{1}$$

$$\frac{\partial u}{\partial t} + u\frac{\partial u}{\partial x} + v\frac{\partial u}{\partial y} = \frac{\mu_{hnf}}{\rho_{hnf}}\frac{\partial^2 u}{\partial y^2} - \frac{\sigma_{hnf}}{\rho_{hnf}}B^2 u, \tag{2}$$

Figure 1 Schematic layout

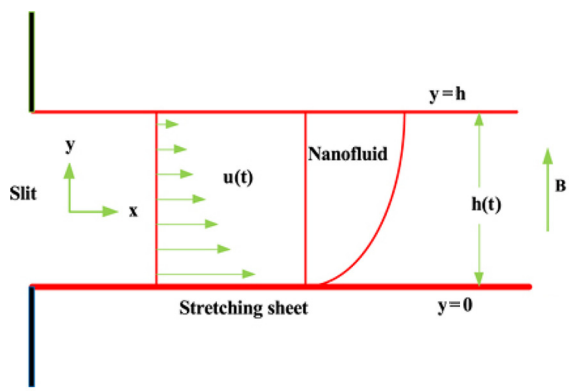

Source: Figure by authors

$$\frac{\partial T}{\partial t}+u\frac{\partial T}{\partial x}+v\frac{\partial T}{\partial y}=\frac{k_{hnf}}{(\rho C_p)_{hnf}}\frac{\partial^2 T}{\partial y^2}. \tag{3}$$

The boundary constraints pertinent to the analysis are as follows:

$$u=U, v=0, T=T_s,\ \ at\ y=0, \tag{4}$$

$$\frac{\partial u}{\partial y}=0,\quad \frac{\partial T}{\partial y}=0,\ \ v=\frac{dh}{dt}\ \ at\ y=h(t). \tag{5}$$

The following scaling analysis was used:

$$\eta=\left[\frac{b}{\nu_f(1-ct)}\right]^{\frac{1}{2}}y\ ,\quad \psi=x\left[\frac{\nu b}{1-ct}\right]^{\frac{1}{2}}f(\eta), \tag{6}$$

$$\theta(\eta)=\frac{T-T_0}{T_S-T_0},\quad T_s\ (x,t)=T_0-T_{ref}\left[\frac{bx^2}{2\nu_f}\right](1-ct)^{-3/2}. \tag{7}$$

We introduce $\psi(x,y)$ such that:

$$u=\frac{\partial \psi}{\partial y}=\frac{bx}{1-ct}f^{'(\eta)},\quad v=-\frac{\partial \psi}{\partial x}=-\left(\frac{\nu_f b}{1-ct}\right)^{1/2}f(\eta) \tag{8}$$

and ξ, the measure of η on the free surface. Thus, ξ can be evaluated with the aid of equation (6) as:

$$\xi=\left(\frac{b}{\nu_f(1-ct)}\right)^{\frac{1}{2}}h(t). \tag{9}$$

In this context, ξ is not known and needs to be determined. Rate of change of the film thickness can be evaluated as given below:

$$\frac{dh}{dt}=-\frac{c\xi}{2}\left(\frac{\nu}{b(1-ct)}\right)^{1/2} \tag{10}$$

Making use of similarity transformation equations (6) and (7), equations (2) and (3) can be expressed, in the finite range of 0 to ξ, as:

$$A_1f'''+A_2\left(ff''-S\left(f'+\frac{\eta}{2}f''\right)-f'2\right)-A_3Mf'=0, \tag{11}$$

$$A_4\theta''+PrA_5\left(f\theta'-2f'\theta-\frac{S}{2}\left(3\theta+\eta\theta'\right)\right)=0, \tag{12}$$

with conditions:

$$f(0)=0,\ f'(0)=1,\ \ \theta(0)=1, \tag{13}$$

$$f(\xi)=\frac{1}{2}S\xi,\ f''(\xi)=0,\ \ \theta'(\xi)=0, \tag{14}$$

where

$$A_1=\frac{\mu_{hnf}}{\mu_f}=\frac{1}{[(1-\phi_1)(1-\phi_2)]^{2.5}},$$

$$A_2=\frac{\rho_{hnf}}{\rho_f}=\left[1-\phi_1+\frac{\rho_{s1}}{\rho_f}\phi_1\right](1-\phi_2)+\frac{\rho_{s2}}{\rho_f}\phi_2,$$

$$A_3=\frac{\sigma_{hnf}}{\sigma_f}=\frac{\sigma_{s2}+(S_f-1)\sigma_{nf}-(S_f-1)\phi_2(\sigma_{nf}-\sigma_{s2})}{\sigma_{s2}+(S_f-1)\sigma_{nf}+\phi_2(\sigma_{nf}-\sigma_{s2})}$$
$$*\frac{\sigma_{s1}+(S_f-1)\sigma_f-(S_f-1)\phi_1(\sigma_f-\sigma_{s1})}{\sigma_{s1}+(S_f-1)\sigma_f+\phi_1(\sigma_f-\sigma_{s1})},$$

$$A_4=\frac{k_{hnf}}{k_f}=\frac{k_{s2}+(S_f-1)k_{nf}-(S_f-1)\phi_2(k_{nf}-k_{s2})}{k_{s2}+(S_f-1)k_{nf}+\phi_2(k_{nf}-k_{s2})}$$
$$*\frac{k_{s1}+(S_f-1)k_f-(S_f-1)\phi_1(k_f-k_{s1})}{k_{s1}+(S_f-1)k_f+\phi_1(k_f-k_{s1})},$$

$$A_5=\frac{(\rho C_p)_{hnf}}{(\rho C_p)_f}=\left[1-\phi_1+\phi_1\frac{(\rho C_p)_{s1}}{(\rho C_p)_f}\right](1-\phi_2)$$
$$+\frac{(\rho C_p)_{s2}}{(\rho C_p)_f}\phi_2. \tag{15}$$

Surface friction coefficient Cf and Nu are presented as given below:

$$Cf_xRe_x^{1/2}=\frac{\mu_{hnf}}{\mu_f}f''(0),\ \ Nu_xRe_x^{-\frac{1}{2}}=-\frac{k_{hnf}}{k_f}\theta'(0),$$

$$\text{and}\qquad Cf=Cf_xRe_x^{1/2},\ \ Nu=Nu_xRe_x^{-1/2} \tag{16}$$

3. Solution methodology

The differential equations described by equations (11) and (12) are nonlinear, making it impractical to derive analytical solutions. Therefore, we used a dual strategy involving both the Runge–Kutta–Fehlberg (RKF) method and shooting techniques simultaneously to compute solutions for the variables f and θ. These equations are converted into a set of equations of order one as mentioned below:

$$\frac{df_0}{d\eta}=f_1, \tag{17}$$

$$\frac{df_1}{d\eta}=f_2, \tag{18}$$

$$A_1\frac{df_2}{d\eta}+A_2\left(f_0f_2-S\left(f_1+\frac{\eta}{2}f_2\right)-f_1^2\right)-A_3Mf_1=0, \tag{19}$$

$$\frac{d\theta_0}{d\eta}=\theta_1, \tag{20}$$

$$A_4\frac{d\theta_1}{d\eta}+PrA_5\left(\theta_1f_0-2\theta_0f_1-\frac{S}{2}(3\theta_0+\eta\theta_1)\right)=0. \tag{21}$$

The associated boundary conditions take the form:

$$f_0(0) = 0, f_1(0) = 1, \ \theta_0 = 1, \tag{22}$$

$$f_0(\xi) = \frac{1}{2}S\xi, f_2(\xi) = 0, \ \theta_1(\xi) = 0. \tag{23}$$

Here, $f_0(\eta) = f(\eta)$ and $\theta_0(\eta) = \theta(\eta)$.

Initial values $f_2(0)$, $\theta_1(0)$ are required for this process, hence appropriate guess values are selected, followed by integration. A step size of $\Delta\eta = 0.01$ is used. The value of ξ is determined such that the boundary constraint $f_0(\xi) = \frac{s\xi}{2}$ is satisfied within an error tolerance of 10^{-6}. The computed results are compared with those obtained by Wang (2006), Abel *et al.* (2009) and Narayana and Sibanda (2012) as a special case, $M = \phi_1 = \phi_2 = 0$. Their consensus is apparent and reliable and is summarized in Table 1.

4. Results and discussions

In this section, flow velocity and fluid temperature plots, skin friction coefficient and local Nusselt number of the HNF (Cu-Al_2O_3) and MNF (Cu/H_2O) are analyzed eliciting the impact of the flow parameters. Throughout the discussion, the physical parameters remain constant, with $M = 1.0$, $S = 0.8$, $Pr = 2.0$ and $S_f = 3.0$, except when variations in these parameters are explored, and such values are illustrated in the corresponding graphs and tables. Further, the base values pertaining to the thermophysical attributes of the host fluid and the nano-sized particles are shown in Tables 2 and 3. Further, the solid plots represent Cu-H_2O nanofluid and dashed plots correspond to the Cu-Al_2O_3/H_2O hybrid nanofluid. Recent experimental investigations ascertained that the use of hybrid nanomaterial in place of mono nanomaterials in the preparation of NFs yields outstanding enhancement of rate of heat transfer (RHT) in hybrid nanofluids relative to a single nanofluid. This is because of the fact that the dual nanoparticles possess very high TC than that of the mono particles. In conformity with this fact in the current investigation for all the variations of the physical parameters the velocities and temperatures of the Cu-Al_2O_3-H_2O fluid are higher than those of Cu-H_2O fluid.

It is appropriate to emphasize that the solutions of thin film problem are valid within the range $0 \leq S \leq 2.0$. The case $S \to 0$ corresponds to $\xi \to \infty$, which refers to a thick fluid layer. In this case, we get the analytical solutions of the problem studied by

Table 3 Thermophysical properties of fluid and nanoparticles (Raza *et al.*, 2016 and Yashkun *et al.*, 2021)

Properties	H_2O	Cu	Al_2O_3
ρ(kg/m^3)	997.1	8,933	3,970
C_p(J/kgK)	4,179	385	765
σ (S/m)	0.05	5.96×10^7	3.69×10^7
k (W/mK)	0.613	400	40

Source: Table by authors

Table 1 Validation of the results for $f''(0)$ when $M = \phi_1 = \phi_2 = 0$ for various values of S

	Wang (2006)		Abel *et al.* (2009)		Narayana and Sibanda (2012)		Present study	
S	ξ	$f''(0)\xi$	ξ	$f''(0)$	ξ	$\xi f''(0)$	ξ	$f''(0)$
0.4	5.122490	−1.307785	4.981455	−1.134098	4.981455	−5.6494483	4.981455	−1.134098
0.6	3.131250	−1.195155	3.131710	−1.195128	3.131713	−3.7427896	3.131710	−1.195128
0.8	2.151990	−1.245795	2.151990	−1.245805	2.151994	−2.6809660	2.151990	−1.245805
1.0	2.543620	−1.277762	1.543617	−1.277769	1.543618	−1.9723877	1.543617	−1.277769
1.2	1.127780	−1.279177	1.127780	−1.279171	1.127780	−1.4426237	1.127780	−1.279171
1.4	0821032	−1.233549	0.821033	−1.233545	0.821032	−1.0127798	0.821033	−1.233545
1.6	0.576173	−1.491137	0.576176	−1.114937	0.576173	−0.6423970	0.576176	−1.114937
1.8	0.356389	−0.867414	0.356390	−0.867416	0.356389	−0.3091369	0.356390	−0.867416

Source: Table by authors

Table 2 Thermophysical properties pertaining to NF and hybrid NF (Yashkun *et al.*, 2021)

Properties	Nanofluids	Hybrid nanofluids
Density	$\rho_{nf} = (1-\phi_1)\rho_f + \phi_1\rho_{s1}$	$\rho_{hnf} = (1-\phi_2)[(1-\phi_1)\rho_f + \phi_1\rho_{s1}] + \phi_2\rho_{s2}$
Heat capacity	$(\rho C_p)_{nf} = (1-\phi_1)(\rho C_p)_f + \phi_1(\rho C_p)_{s1}$	$(\rho C_p)_{hnf} = (1-\phi_2)\left[(1-\phi_1)(\rho C_p)_f + \phi_1(\rho C_p)_{s1}\right] + \phi_2(\rho C_p)_{s2}$
Dynamic viscosity	$\mu_{nf} = \frac{\mu_f}{(1-\phi_1)^{2.5}}$	$\mu_{hnf} = \frac{\mu_f}{(1-\phi_1)^{2.5}(1-\phi_2)^{2.5}}$
Electrical conductivity	$\sigma_{nf} = 1 + \frac{3\left(\frac{\sigma_{s1}}{\sigma_f} - 1\right)\phi_1}{2 + \frac{\sigma_{s1}}{\sigma_f} - \left(\frac{\sigma_{s1}}{\sigma_f} - 1\right)\phi_1} * \sigma_f$	$\sigma_{hnf} = \frac{\sigma_{s2} + (S_f-1)\sigma_{nf} - (S_f-1)\phi_2(\sigma_{nf} - \sigma_{s2})}{\sigma_{s2} + (S_f-1)\sigma_{nf} + \phi_2(\sigma_{nf} - \sigma_{s2})} * \sigma_{nf}$
Thermal conductivity	$k_{nf} = \frac{k_{s1} + (S_f-1)k_f - (S_f-1)\phi_1(k_f - k_{s1})}{k_{s1} + (S_f-1)k_f + \phi_1(k_f - k_{s1})} * k_f$	$k_{hnf} = \frac{k_{s2} + (S_f-1)k_{nf} - (S_f-1)\phi_2(k_{nf} - k_{s2})}{k_{s2} + (S_f-1)k_{nf} + \phi_2(k_{nf} - k_{s2})} * k_{nf}$

Source: Table by authors

Crane (1970). Alternatively, as S→2.0, it signifies another limiting solution indicating a film of infinitesimal thickness ($\xi \to \infty$). The results are derived and deliberated for $0 \leq S \leq 2.0$ *and* $0 \leq \phi_1, \phi_2 \leq 0.2$.

Figure 2 presents the effect of S on ξ, film thickness in both phases of liquids. The fluid layer evidently extends infinitely in width as $S \to 0$, and its thickness diminishes to 0 for $\to 2$. These findings are consistent with facts presented in the preceding paragraph. It is found that hybrid nanoliquid has a greater film thickness than the Cu-H_2O fluid.

Figure 3 reveals the relationship between the fluid velocity f' and S throughout the film. An increase in S leads to the enhancement of velocity of both phases. There is a notable rise in the velocity at the free surface. As S range s from 0.8 to 1.4, velocity at the free surface in the Cu-H_2O fluid experiences 211% enhancement while in the hybrid phase, the enhancement reaches 212%. For higher measures of S, film thickness is dwindled in both fluids and, consequently, thinner boundary layers prevail. Figure 4 depicts the behavior of temperature θ against S. Temperature similarly tracks the trend of velocity for the same range of S. As S ranges from 0.8 to 1.2, the temperature of the dual fluid elevates by 234%, whereas the monoNF undergoes a rise of 200%.

Figures 5 and 6 elicit the nature of f' and θ for varying strengths of magnetic field through M. Increasing M results in reduced velocities on account of the resistance offered by Lorentz force to the flow in the film. Higher intensities in the magnetic field cause further reduction in velocity. The temperature has a reversal trend. This may be attributed to the generation of frictional drag caused by the Lorentz force, resulting in increased heat dissipation and a subsequent rise in temperature.

Effect of ϕ_1 on f' and θ is illustrated in Figures 7 and 8. Increase in ϕ_1 caused a decline in velocities of both phases. This

Figure 2 Variation of S and ξ for different values of ϕ_2

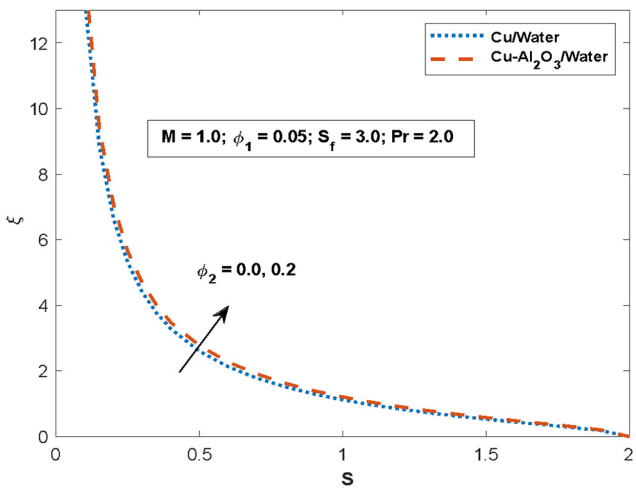

Source: Figure by authors

Figure 3 Variation of S on f'

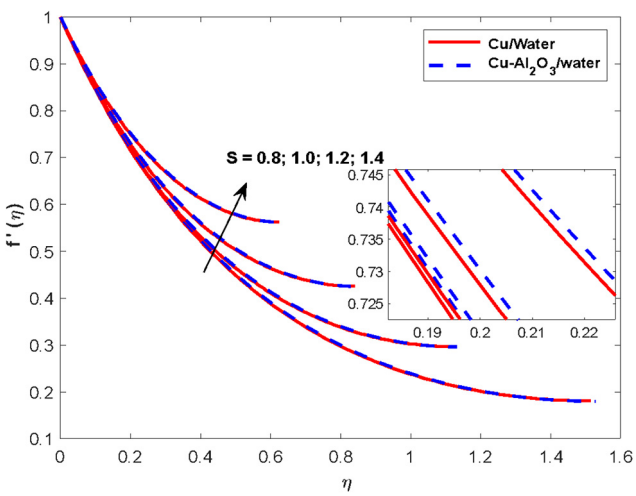

Source: Figure by authors

Figure 4 Variation of S on θ

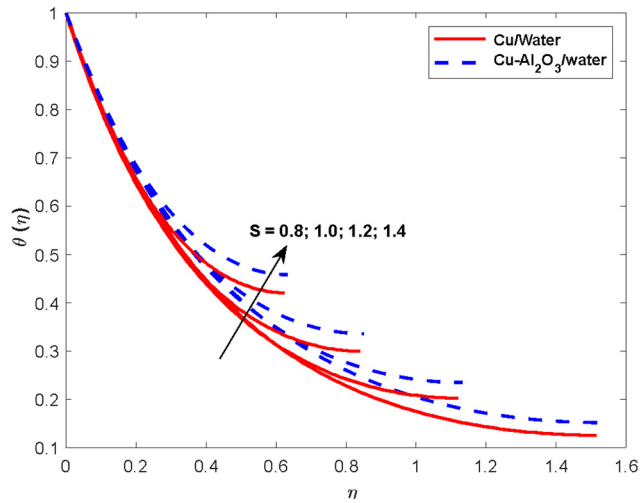

Source: Figure by authors

Figure 5 Variation of M on f'

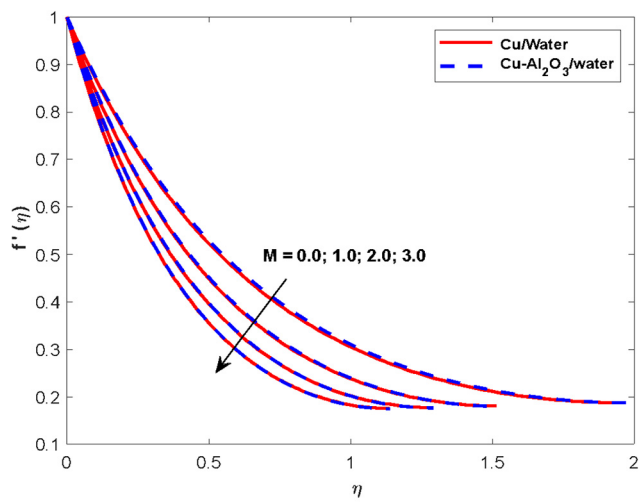

Source: Figure by authors

Figure 6 Variation of M on θ

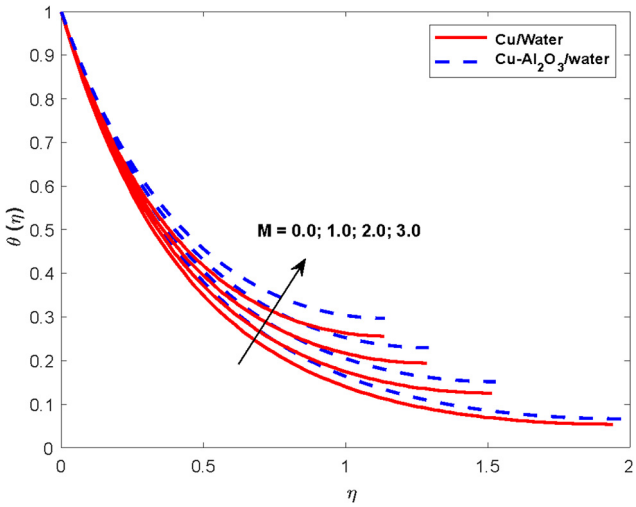

Source: Figure by authors

Figure 7 Variation of ϕ_1 on f'

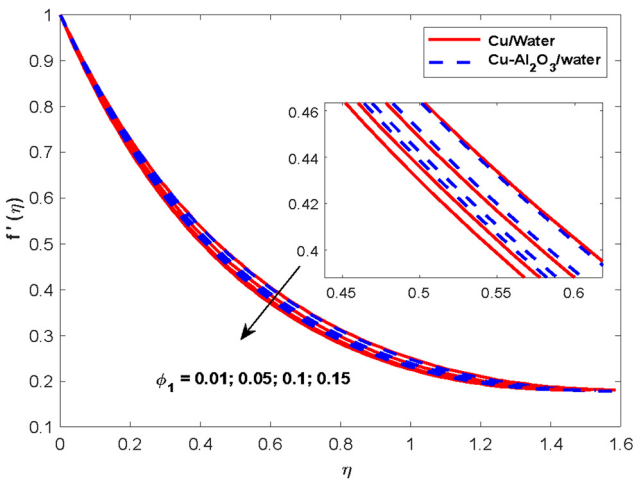

Source: Figure by authors

Figure 8 Variation of ϕ_1 on θ

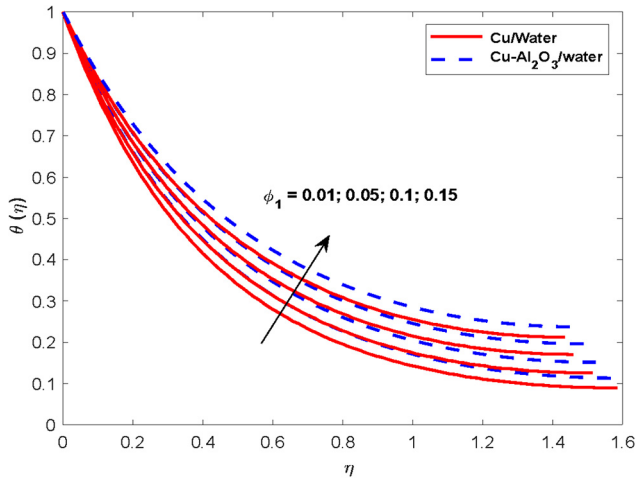

Source: Figure by authors

Figure 9 Variation of S_f on f'

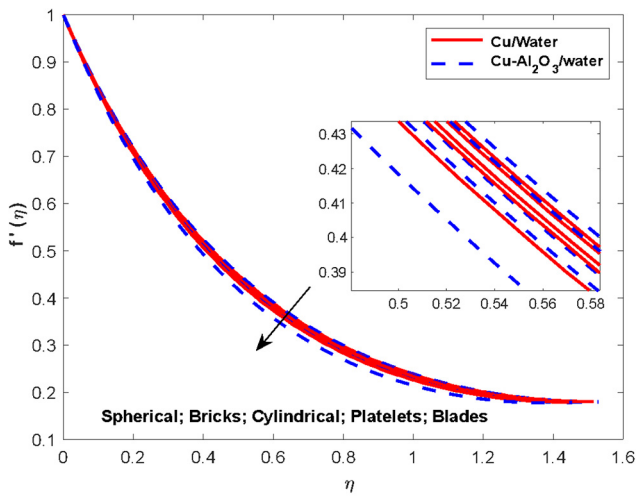

Source: Figure by authors

may be explained that larger number particles of Cu cause an increase in the viscosity of the liquids which is responsible for a slight abatement in velocity. At the same time, temperature across the film is heightened with increased ϕ_1 as Cu particles contain higher TC that facilitates appreciable thermal energy transport.

Figures 9 and 10 are drawn to infer the behavior of f' and θ to S_f(shape factor). Nanoparticles of different geometries, i.e. spheres ($S_f = 3.0$), bricks ($S_f = 3.7$), cylinders ($S_f = 4.9$), platelets ($S_f = 5.7$) and blades ($S_f = 8.6$) are reckoned. It is interesting to note that the velocity of HNF is greater than that nanofluid with copper particles when spherical and brick-shaped particles are used. However, the cylindrical, platelet and blade-shaped particles enhance the velocity of the MNF relative to that of the hybrid nanofluid. This may be ascribed to the smaller surface area of spherically and brick-shaped particles. In both phases, the velocity declines with increased shape factor. When two nanomaterials Cu and Al_2O_3 are spherically shaped, the temperature and the RHT are lowest. However, the thermal measure of nanofluid is relatively higher when using cylindrical shaped particles than when using spherical case. The temperature is further raised by particles in the shape of platelets. Presence of blade-shaped nanomaterials yields the highest temperature and thus the greater RHT. This can be explained by the fact that the blades possess a greater surface area than other geometries, which facilitates stronger TC. Hence, the shape factor has a significant role in achieving the highest rates of thermal transmission.

Figure 11 reveals the relationship between Pr and θ. It is noticed that smaller measures of Pr yield higher temperatures in both the fluids owing to the fact that enhanced values of Pr

Figure 10 Variation of S_f on θ

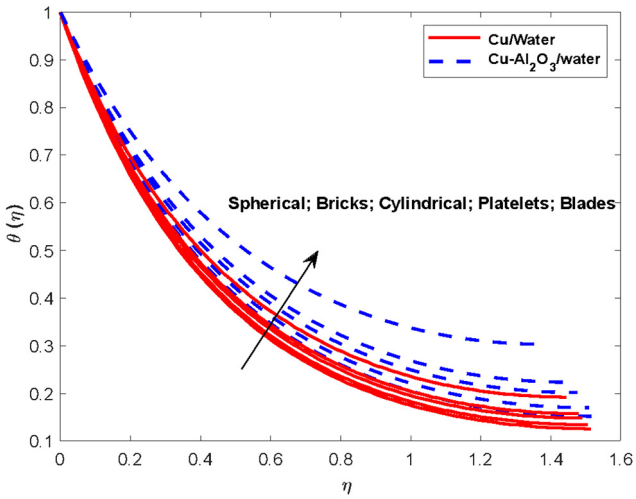

Source: Figure by authors

Figure 11 Variation of Pr on θ

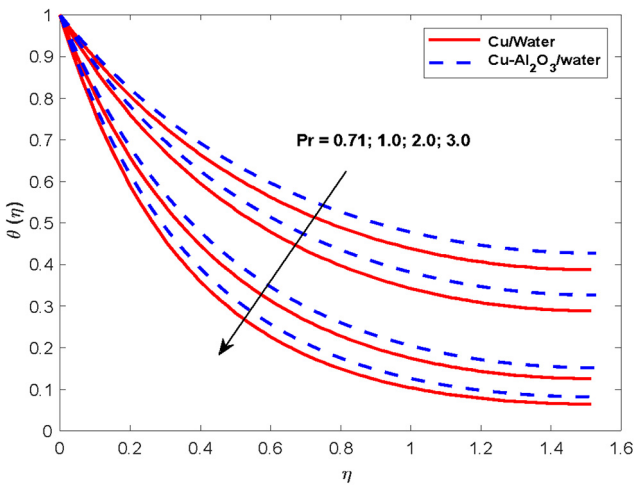

Source: Figure by authors

Figure 12 Variation of S_f and Pr on $Nu_x/Re_x^{1/2}$ with MNF

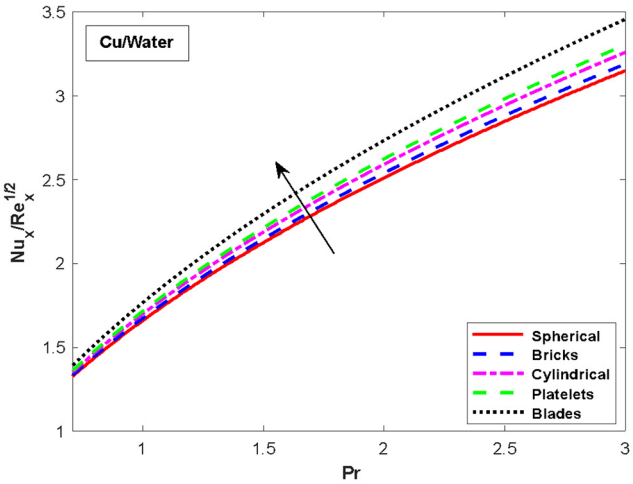

Source: Figure by authors

Figure 13 Variation of S_f and Pr on $Nu_x/Re_x^{1/2}$ with hybrid nanofluid

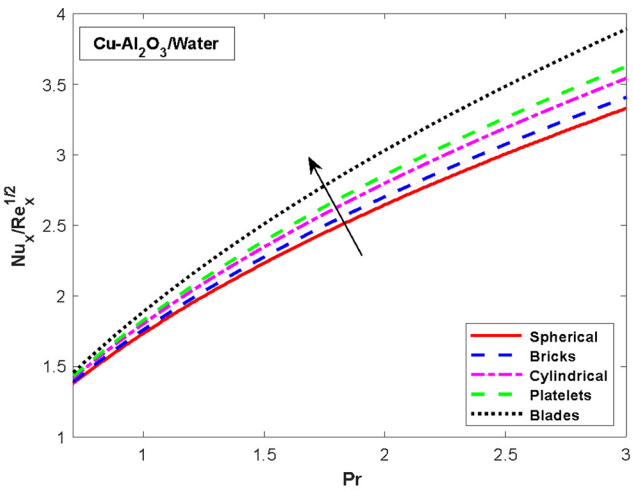

Source: Figure by authors

indicate lesser TC. For higher measures of Pr values, thinner thermal boundary layers are formed.

Figures 12 and 13 are the plots of Nusselt number Nu versus Pr drawn for distinct shapes of dispersed nanomaterials representing hybrid and MNFs, respectively. At $Pr = 2.0$, hybrid nanofluid with brick-shaped Cu and Al_2O_3 nanoparticles exhibited a 2.27% enhancement in RHT compared to spherical-shaped nanomaterials, while in the Cu-H_2O nanofluid, the corresponding enhancement was 1.25%. Likewise, there is an enhancement with cylindrical and platelet-shaped nanoparticles. The RHT in hybrid nanofluid is appreciably enhanced by 14.7% with blade-shaped nanoparticles compared to the spherical-shaped particles and 8.98% is the corresponding enhancement in the Cu-H_2O nanofluid.

Table 4 presents the film thickness, C_f, Nu and free surface temperature $[\theta(\xi)]$in Cu/H_2O and Cu-Al_2O_3/H_2O fluids, for variations in all physical parameters. In the variations of all parameters, the film thickness of the Cu-Al_2O_3/H_2O fluid is higher than the Cu/H_2O fluid. However, with cylinder, platelets and blade-shaped nanoparticles, the thickness of the film of MNFs overshadows the associated values of hybrid nanofluids. The values of C_f and Nu pertaining to the two nanofluids varying S, M, ϕ_1, S_f *and* Pr are tabulated. For all the variations in S, M, ϕ_1 *and* S_f the numerical values of the drag coefficient of Cu-Al_2O_3-H_2O fluid are higher than the corresponding Cu-H_2O nanofluid. In the two phases, the drag coefficient is enhanced with augmented values of S while a reversal trend prevails with M, ϕ_1 *and* S_f. The Nusselt number is augmented with increased S_f and volume fraction

Table 4 Values of $A_1 f''(0)$ *and* $-A_4\theta'(0)$ and $\theta(\xi)$ for $Cu-H_2O$ and $Cu-Al_2O_3-H_2O$

					$A_1 f''(0)$		$-A_4\theta'(0)$		$\theta(\xi)$	
S	**M**	ϕ_1	S_f	**Pr**	$Cu-H_2O$	$Cu-Al_2O_3-H_2O$	$Cu-H_2O$	$Cu-Al_2O_3-H_2O$	$Cu-H_2O$	$Cu-Al_2O_3-H_2O$
0.8	1.0	0.05	3.0	2.0	*−1.936245*	*−2.179723*	*2.509338*	*2.645621*	*0.125780*	*0.152261*
1.0					−1.950038	−2.193695	2.608657	2.745172	0.202589	0.235164
1.2					−1.919436	−2.157780	2.672454	2.801368	0.299745	0.336426
1.4					−1.822628	−2.047617	2.669464	2.780479	0.420617	0.458443
	0.0				−1.570476	−1.750121	2.576923	2.728955	0.054249	0.067096
0.8	*1.0*		3.0	2.0	*−1.936245*	*−2.179723*	*2.509338*	*2.645621*	*0.125780*	*0.152261*
	2.0				−2.242668	−2.537052	2.445288	2.566264	0.194648	0.230240
	3.0	0.05			−2.511837	−2.849758	2.383499	2.490313	0.256351	0.297628
		0.01			−1.657201	−1.889977	2.410337	2.542280	0.089727	0.114017
0.8	1.0	*0.05*	3.0	2.0	*−1.936245*	*−2.179723*	*2.509338*	*2.645621*	*0.125780*	*0.152261*
		0.1			−2.306087	−2.569017	2.633475	2.774896	0.170910	0.197020
		0.15			−2.710930	−2.998783	2.759995	2.906425	0.212795	0.237878
0.8	1.0	0.05	*3.0*	2.0	*−1.936245*	*−2.179723*	*2.509338*	*2.645621*	*0.125780*	*0.152261*
			3.7		−1.946743	−2.204587	2.540758	2.705682	0.133909	0.170167
			4.9		−1.964608	−2.248333	2.592358	2.801201	0.148008	0.201937
			5.7		−1.976427	−2.278251	2.625233	2.859536	0.157495	0.223646
			8.6		−2.018689	−2.391361	2.734877	3.034740	0.192185	0.303464
				0.71			1.326067	1.377483	0.387447	0.427899
				1.0			1.658149	1.732868	0.288575	0.326927
0.8	1.0	0.05	3.0	*2.0*	*−1.936245*	*−2.179723*	*2.509338*	*2.645621*	*0.125780*	*0.152261*
				3.0			3.148705	3.329257	0.064371	0.081994

Source: Table by authors

ϕ_1 while an opposite effect is noticed with M. It is evident that the free surface temperature of the HNF dominates that of MNF for all variations. The temperature at the free surface enhances for all variations of M, ϕ_1 *and* S_f in both fluids while the opposite is noticed with Pr.

4.1 Strengths and limitations

The present investigation suggests that scientists choose the appropriate shape of the nanoparticles to yield the maximum TC enhancing the rate of thermal transmission in thin film flows. Owing to the assumption that the magnetic Reynolds number is small, the induced effects of MgF could not be taken into account.

5. Conclusions

In this research work, flow and thermal energy transmission of the nanofluids Cu-Al_2O_3/H_2O and Cu/H_2O within a slender film on an elongated surface under the impact of MgF is examined using RKF algorithm combined with a shooting technique. A gist of the salient features is given here under:

- Velocity profiles of both fluids under study show a declination with M, ϕ_1 and S_f while it rises with S.
- The temperature of the Cu-Al_2O_3/H_2O fluid is higher than that of the Cu-H_2O fluid.
- Temperature in both fluids is enhanced with S, M, ϕ_1 and S_f while an opposite trend with Pr is noticed.
- Skin friction at the boundary increases with S and reduces with M.
- Temperature has a promising impact for shape factor and concentration of nanoparticles.
- Temperature at the free surface follows the same trend of temperature for all the variations of flow parameters.

It is confidently expressed that the current analysis provides a solid foundation for the identification of shape of the nanoscale particles and the nanoliquid that facilitate high TC and thereby increasing heat transmission.

Future scope: This study can be further refined by extending this analysis to ternary nanofluids and considering other significant factors such as viscous dissipation, heat generation and thermal radiation which facilitate further enhancement of TC. Non-Newtonian fluids can be considered for base fluid.

References

Abel, M.S., Mahesha, N. and Tawade, J. (2009), "Heat transfer in a liquid film over an unsteady stretching surface with viscous dissipation in presence of external magnetic field", *Applied Mathematical Modelling*, Vol. 33 No. 8, pp. 3430-3441.

Adil Sadiq, M. (2021), "Heat transfer of a nanoliquid thin film over a stretching sheet with surface temperature and internal heat generation", *Journal of Thermal Analysis and Calorimetry*, Vol. 143 No. 3, pp. 2075-2083.

Alharbi, A.F., Alhawiti, M., Usman, M. and Ullah, I. (2024), "Enhancement of heat transfer in thin-film flow of a hybrid nanofluid over an inclined rotating disk subject to thermal radiation and viscous dissipation", *International Journal of Heat and Fluid Flow*, Vol. 107, p. 1054.

Anantha Kumar, K., Sandeep, N., Sugunamma, V. and Animasaun, I.L. (2019), "Effect of irregular heat source/sink on the radiative thin film flow of MHD hybrid ferrofluid",

Journal of Thermal Analysis and Calorimetry, Vol. 139 No. 3, pp. 2145-2153.

Bachok, N., Ishak, A. and Pop, I. (2010), "Boundary layer flow of nanofluids over a moving surface in a flowing fluid", *International Journal of Thermal Sciences*, Vol. 49 No. 9, pp. 1663-1668.

Bachok, N., Ishak, A. and Pop, I. (2012), "Boundary layer stagnation – point flow and heat transfer over an exponentially stretching/shrinking sheet in a nanofluid", *International Journal of Heat and Mass Transfer*, Vol. 55 Nos 25/26, pp. 8122-8128.

Bhatti, M.M., Öztop, H.F. and Ellahi, R. (2022), "Study of the magnetized hybrid nanofluid flow through a flat elastic surface with applications in solar energy", *Materials*, Vol. 15 No. 21, p. 7507.

Buongiorno, J. (2006), "Convective transport in nanofluids", *Journal of Heat Transfer*, Vol. 128 No. 3, pp. 240-250.

Buongiorno, J. and Hu, L.W. (2010), "Nanofluid heat transfer enhancement for nuclear reactor applications", *Journal of Energy and Power Engineering*, Vol. 4, pp. 1-8.

Choi, S.U.S. and Eastman, J.A. (1995), "Enhancing thermal conductivity of fluids with nanoparticles", ASME Publications-Fed, Vol. 231, pp. 99-106.

Crane, L.J. (1970), "Flow past a stretching plate", *ZAMP*, Vol. 21, pp. 645-647.

Devi, S.P.A. and Devi, S.S.U. (2016), "Numerical investigation of hydromagnetic hybrid Cu–Al2O3/water nanofluid flow over a permeable stretching sheet with suction", *International Journal of Nonlinear Sciences and Numerical Simulation*, Vol. 17 No. 5, pp. 249-257.

Devi, S.U. and Devi, S.P.A. (2017), "Heat transfer enhancement of Cu–Al2O3/water hybrid nanofluid flow over a stretching sheet", *Journal of the Nigerian Mathematical Society*, Vol. 36, pp. 419-433.

Eastman, J.A., Choi, S.U.S., Li, S., Yu, W. and Thompson, L. J. (2001), "Anomalously increased effective thermal conductivities of ethylene glycol based nano fluids containing coper nanoparticles", *Applied Physics Letters*, Vol. 78 No. 6, pp. 718-720.

Ghadikolaei, S.S., Gholinia, M., Hoseini, M.E. and Ganji, D. D. (2019), "Natural convection MHD flow due to MoS2–Ag nanoparticles suspended in C2H6O2H2O hybrid base fluid with thermal radiation", *Journal of the Taiwan Institute of Chemical Engineers*, Vol. 97, pp. 12-23.

Ghadikolaei, S.S., Hosseinzadeh, K., Hatami, M. and Ganji, D.D. (2018), "MHD boundary layer analysis for micropolar dusty fluid containing hybrid nanoparticles (Cu-Al 2 O 3 over a porous medium", *Journal of Molecular Liquids*, Vol. 268, pp. 813-823.

Gul, T., Bilal, M., Shuaib, M., Mukhtar, S. and Thounthong, P. (2020), "Thin film flow of the water-based carbon nanotubes hybrid nanofluid under the magnetic effects", *Heat Transfer*, Vol. 49 No. 6, pp. 3211-3227.

Hassan, M., Marin, M., Ellahi, R. and Alamri, S.Z. (2018), "Exploration of convective heat transfer and flow characteristics synthesis by Cu–Ag/water hybrid-nanofluids", *Heat Transfer Research*, Vol. 49 No. 18, pp. 1837-1848.

Jana, S., Salehi-Khojin, A. and Zhong, W.H. (2007), "Enhancement of fluid thermal conductivity by the addition of single and hybrid nano-additives", *Thermochimica Acta*, Vol. 462 Nos 1/2, pp. 45-55.

Jazaa, Y., Rehman, S. and Albouchi, F. (2024), "On the enhancement of heat transport and entropy generation of the thin film flow of partially ionized non-Newtonian hybrid nanofluid", *Journal of the Taiwan Institute of Chemical Engineers*, Vol. 157, p. 105412.

Khan, W.A. and Pop, I. (2010), "Boundary layer flow of a nanofluid past a stretching sheet", *International Journal of Heat and Mass Transfer*, Vol. 53 Nos 11/12, pp. 2477-2483.

Leong, L.S., Basir, M.F.M., Jaafar, N.A., Chaharborj, S.S., Khairuddin, T.K.A. and Naganthran, K. (2020), "Numerical solutions for the thin film hybrid nanofluid flow and heat transfer over an unsteady stretching sheet", *Open Journal of Science and Technology*, Vol. 3 No. 4, pp. 335-344, doi: 10.31580/ojst.v3i4.1674.

Manjunatha, S., Ammani Kuttan, B., Jayanthi, S., Chamkha, A. and Gireesha, B.J. (2019), "Heat transfer enhancement in the boundary layer flow of hybrid nanofluids due to variable viscosity and natural convection", *Heliyon*, Vol. 5 No. 4, p. e01469.

Megahed, A.M. (2015), "Effect of slip velocity on Casson thin film flow and heat transfer due to unsteady stretching sheet in presence of variable heat flux and viscous dissipation", *Applied Mathematics and Mechanics*, Vol. 36 No. 10, p. 1273.

Nadeem, S. and Awais, M. (2008), "Thin film flow of an unsteady shrinking sheet, through medium with variable viscosity", *Physics Letters A*, Vol. 372 No. 30, pp. 4965-4972.

Nadeem, S., Haq, R.U. and Khan, Z.H. (2014), "Heat transfer analysis of water – based nanofluid over an exponentially stretching sheet", *Alexandria Engineering Journal*, Vol. 53 No. 1, pp. 219-224.

Narayana, M. and Sibanda, P. (2012), "Laminar flow of a nanoliquid film over an unsteady stretching sheet", *International Journal of Heat and Mass Transfer*, Vol. 55 Nos 25/26, pp. 7552-7560.

Raza, J., Rohni, A.M. and Omar, Z. (2016), "Numerical investigation of copper-water (Cu-water) nanofluid with different shapes of nanoparticles in a channel with stretching wall: slip effects", *Mathematical and Computational Applications*, Vol. 21 No. 4, p. 43.

Sarojamma, G., Vajravelu, K. and Sreelakshmi, K. (2017), "A study on entropy generation on thin film flow over an unsteady stretching sheet under the influence of magnetic field, thermocapillarity, thermal radiation and internal heat generation/absorption", *Communications in Numerical Analysis*, Vol. 2017 No. 2, pp. 141-156.

Selimefendigil, F. and Oztop, H.F. (2023), "Combined effects of using multiple porous cylinders and inclined magnetic field on the performance of hybrid nanoliquid forced convection", *Journal of Magnetism and Magnetic Materials*, Vol. 565, p. 170137.

Sheikholeslami, M. and Sadoughi, M.K. (2018), "Simulation of CuO-water nano fluid heat transfer enhancement in presence of melting surface", *International Journal of Heat and Mass Transfer*, Vol. 116, pp. 909-919.

Sreelakshmi, K. and Sarojamma, G. (2018), "Effect of thermocapillarity and variable thermal conductivity on the heat transfer analysis of a non-Newtonian liquid thin film over a stretching surface in the presence of thermal radiation and heat source/sink", *Nonlinear Engineering*, Vol. 7 No. 2, pp. 151-161.

Sreelakshmi, K., Sarojamma, G. and Vajravelu, K. (2019), "Effect of thermophoresis and Brownian motion on the melting heat transfer of a Jeffrey fluid near a stagnation point towards a stretching surface: Buongiorno's model", *Heat Transfer*, Vol. 48 No. 7, pp. 3328-3349.

Thamizhselvi, V., Srilakshmi, K., Sarojamma, G. and Vajravelu, K. (2023), "Darcy-Forchheimer hybrid nanofluid flow in an asymmetric channel with an exponential heat source, variable thermal conductivity, and activation energy", *Numerical Heat Transfer Applications*, Vol. 23pp, pp. 21-34.

Tiwari, R.K. and Das, M.K. (2007), "Heat transfer augmentation in a two-sided lid-driven differentially heated square cavity utilizing nanofluids", *International Journal of Heat and Mass Transfer*, Vol. 50 Nos 9/10, pp. 2002-2018.

Turcu, R., Darabont, A., Nan, A., Aldea, N., Macovei, D., Bica, D. and Vekas, L. (2006), "New polypyrrole-multiwall carbon nanotubes hybrid materials", *Journal of Optoelectronics and Advanced Materials*, Vol. 8 No. 2, pp. 643-647.

Ullah, A., Alzahrani, E., Shah, Z., Ayaz, M. and Islam, S. (2018), "Nanofluids thin film flow of Reiner-Philippoff fluid over an unstable stretching surface with Brownian motion and thermophoresis effects", *Coatings*, Vol. 9 No. 1, pp. 1-20.

Vajravelu, K., Prasad, K.V. and Ng, C. (2012), "Unsteady flow and heat transfer in a thin film of Ostwald–de Waele liquid over a stretching surface", *Communications in Nonlinear Science and Numerical Simulation*, Vol. 17 No. 11, pp. 4163-4173.

Veera Krishna, M., Ameer Ahammad, N. and Chamkha, A.J. (2021), "Radiative MHD flow of Casson hybrid nanofluid over an infinite exponentially accelerated vertical porous surface", *Case Studies in Thermal Engineering*, Vol. 27, p. 101229.

Wang, C. (2006), "Analytical solutions for a liquid film on an unsteady stretching surface", *Heat and Mass Transfer*, Vol. 42 No. 8, pp. 759-766.

Wang, C.Y. (1990), "Liquid film on an unsteady stretching surface", *Quarterly of Applied Mathematics*, Vol. 48 No. 4, pp. 601-610.

Xu, H., Pop, I. and You, X.-C. (2013), "Flow and heat transfer in a nano-liquid film over an unsteady stretching surface", *International Journal of Heat and Mass Transfer*, Vol. 60, pp. 646-652.

Yashkun, U., Zaimi, K., Ishak, A., Pop, I. and Sidaoui, R. (2021), "Hybrid nanofluid flow through an exponentially stretching/shrinking sheet with mixed convection and Joule heating", *International Journal of Numerical Methods for Heat & Fluid Flow*, Vol. 31 No. 6, pp. 1930-1950.

Corresponding author

Kakanuti Malleswari can be contacted at: malleswarik1989@gmail.com

For instructions on how to order reprints of this article, please visit our website:
www.emeraldgrouppublishing.com/licensing/reprints.htm
Or contact us for further details: **permissions@emeraldinsight.com**